A NEW OPTICAL DESIGN FOR THE GAIA ASTROMETRY MISSION [1]

E. Høg, C. Fabricius, V.V. Makarov

Copenhagen University Observatory
Østervoldgade 3, 1350 Copenhagen K, Denmark

ABSTRACT

An interferometric astrometric mission, aiming at accuracies at around the 10 microarcsec level, was recommended as a high priority concept within the new ESA Horizon 2000+ scientific programme. The original outline concept for such a mission, GAIA, presented its general feasibility but did not address many questions of implementation or optimisation. Another concept of an interferometer for a scanning astrometric satellite is presented. It contains a simpler optical telescope and a more efficient detector system. The design utilizes the full resolution of all light in the dispersed fringes of a Fizeau interferometer. A preliminary optimization of the satellite indicates that two telescope units with a baseline of 100 cm will achieve a precision of 3, 8, 22, 68, 302 microarcsec for parallaxes of stars with $V = 12$, 14, 16, 18, 20 mag, respectively, from a 5 year mission. Simultaneous spectrophotometry of the entire spectrum of each star will be obtained with a resolution corresponding to intermediate band photometry. The expected precision of this photometry is about 0.003 mag for $V = 16$. The performance is good in crowded fields, at least up to one star per 5 arcsec^2. A Hipparcos-type beam combiner of 150 cm width is placed in front of a telescope with 4 square apertures of 50 cm. The assumed focal length is $f = 60$ m and the field 0.5 degree diameter. The detector consists of CCDs used for time delayed integration (drift-scan.)

Keywords: space astrometry; interferometry; spectrophotometry; GAIA

1. INTRODUCTION

The proposed new design builds on the experience from Hipparcos, see e.g., Mignard (1995), in particular, a beam combiner of Hipparcos-type in front of a reflector telescope is adopted. The new proposal combines features from three recent designs of scanning astrometric satellites. The potential of using CCDs in a scanning astrometric satellite was first described for the ROEMER project by Høg (1993). The idea of using a Fizeau interferometer was first proposed for GAIA by Lindegren *et al.* (1994). A realistic design of such an instrument using dispersed fringes and direct fringe detection has been given for the FAME project by Seidelmann *et al.* (1995), Johnston (1995) and in private communications. We shall in the following sometimes refer to the new design of GAIA briefly as GAIA95. The original design was first presented in detail by Lindegren & Perryman (1994) and may be referred to as GAIA94.

The GAIA design was discussed at the RGO-ESA workshop in June 1995 as reported in ESA SP-379. The original design of GAIA is described by Lindegren & Perryman in I2 of SP-379. The proposed detector system with a modulating grid is not very efficient because light is lost in the colour filters required to obtain fringe visibility throughout the stellar image. The use of dispersed fringes and of direct fringe detection was therefore advocated by several speakers (Noordam in C7 of SP-379, Gai *et al.* C10, Daigne C6, Lindegren C15, Casertano E2, Lattanzi E5). But direct fringe detection with the given focal length for the original GAIA would require detectors with pixels of width only 0.5 μm (Lindegren, SP-379-C15) which is much smaller than the state of art for CCDs.

To solve these problems we introduce a new kind of telescope with much longer focal length than the original 11 m and we insert a prism with very low-dispersion (500 nm/mm) in the converging beam. The telescope for FAME also has a long focal length $f = 36$ m and $D = 60$ cm and a field of 0.5 degrees diameter and is built very compactly. But the field can only be used in an annulus from radius 0.15 to 0.33 degrees, and one half of this annulus is furthermore obstructed. The FAME telescope contains six curved aspheric mirrors. A simpler but not so compact design with $f = 60$ m and $D = 150$ cm is proposed in this report, containing only a flat beam combiner, two curved aspheric mirrors, a small field lens and two flat aspheric folding mirrors. This system would fully utilize the astrometric information in the monochromatic fringes if pixels of width 5 μm are used. This width of pixels in a CCD is believed to be a realistic requirement for a future ESA satellite. The dispersed fringes are utilized to obtain spectrophotometric information on all stars. This means that no area of the focal plane is occupied by photometric colour filters as in the original GAIA design and in ROEMER.

Thus, the use of dispersed fringes gives a number of advantages:

1. the full monochromatic structure of all the light is utilized for astrometry and spectrophotometry;

2. no colour filters are absorbing a large fraction of light as required in the original GAIA for coherent imaging on the modulating grid;

[1] Date: **4 Jan. 1996**; changes are listed in Sect. 7.

3. no photometric colour filters occupy focal plane area as in the ROEMER and original GAIA for incoherent imaging, and *all* light is utilized for spectrophotometry, not only some light through colour filters;

4. the light is spread over a larger number of pixels so that saturation of the CCD only occurs at brighter stars;

5. high order spectral fringes give attenuation for bright stars as required for astrometry and spectrophotometry; and

6. the different spectral orders provide a photometric scale which is useful for verification of the linearity of the CCD response.

The problem of dynamic range over more than 15 magnitudes addressed in #4 and #5 had to be solved in several ways in the ROEMER design. Every CCD chip contained a narrow and a wide CCD giving different integration times. The narrow CCDs had longer pixels and therefore a larger area for accumulation of more electron holes. Even so, however, attenuation by the colour filters was required to measure the brightest stars.

The point #4 gives the disadvantage that readout noise (but not sky background) becomes more prominent than in the direct imaging of ROEMER or the original GAIA-incoherent, with a resulting brighter limiting magnitude. But the readnoise is not too serious, see. Sects. 3 and 5.1. The sky area per star of the useful fringes is quite small about 2.5 arcsec^2 per field of view. Stars from the other field will also appear, but this does not matter in crowded fields because only one of the fields will generally be very crowded. So, the 'instantaneous field-of-view' per star is effectively 100 times smaller than the 300 arcsec^2 for a subfield of the original GAIA proposal. Therefore, the new version can measure in crowded fields, in fact even better than ROEMER (Høg SP-379-C13) which touches a sky area about 4 arcsec^2 at each star.

2. TELESCOPE DESIGN

A telescope with a large f-number $\equiv f/D \simeq 40$ is required. The obvious first idea is a Ritchey-Chretien system. This system is aplanatic (i.e., no spherical aberration and no coma) but it has field astigmatism and field curvature. The astigmatism can be compensated by a flat aspheric plate some distance before the focus. Such a system was drafted with the dimensions of the FAME telescope quoted above, but the resulting field curvature was enormous. According to Sect. 18 of Bahner (1967) the radius of curvature would be about $r = -20$ cm allowing a field size of only a few arcminutes. The large intrinsic field curvature of a Ritchey-Chretien system is probably one of the reasons for the rather complicated design for FAME where a flat field is obtained by a relay system with four curved aspheric mirrors.

The telescope for the GAIA95 design in Fig. 1 is basically an aplanatic Gregorian system consisting of the mirrors S2 and S3. Such a system is perfectly aplanatic, that is free of spherical aberration and coma of all orders in the aperture. The remaining aberrations, field astigmatism, distortion and field curvature, are given by Schroeder (1987, Table 6.7). The Petzval field curvature is $r \simeq +41$ cm, convex towards the incoming light. This curvature is compensated by a field lens, L, at the focus of S2 with a focal length about +27 cm. The field lens shifts the exit pupil from where it is shown in Fig. 1d to a position $\simeq 52$ cm behind S3.

The beam combiner S1 is perfectly flat. It needs no Schmidt deformation of the reflecting surface as in Hipparcos. This deformation in Hipparcos was elliptical so as to appear rotationally symmetric from the direction of view lest an axial astigmatism would arize. This posed a difficult manufacturing problem for Hipparcos. When the beam combiner is flat the basic angle may be larger than shown in Fig. 1a, where the value about 60 degrees of Hipparcos is illustrated. About 80 degrees will facilitate the baffling.

The prism P1 gives the dispersion of the interference fringes.

The field astigmatism is -0.416 arcsec and the distortion is 0.193 arcsec, both at a field angle of 18 arcmin. These aberrations are eliminated by the flat aspheric mirrors S4 and S5 in Fig. 1b. These mirrors are tilted by about 6 degrees from the perpendicular direction resulting in an unobstructed field of 0.5 degree diameter, Figs. 1b and 1c.

The dark space between the two interfering beams should have the same width as each beam, i.e., $D/3$ in Fig. 1. It is shown in Sect. 5 that this gives optimal astrometric precision for a given total width D of both beams and D is probably a critical limiting size for a satellite telescope.

2.1. Discussion

The proposed Gregorian system may be considered as a large decollimating telescope and a small almost collimating one. Since the prism is placed in a nearly collimated beam there should be no problems.

An optical design effort is required to verify that the proposal provides diffraction limited images and low distortion in a flat field of about 0.5 degree diameter. Such a field size should be sufficient to ensure rigid great circle solutions when a very smooth rotation can be assumed. This question should be studied, cf. Makarov *et al.* (1995) (Note in this paper that the plots of Figs. 1 and 3 must be interchanged!). In principle, one GAIA95 telescope is sufficient for an astrometric mission, but it is adviceable to incorporate two telescopes with different basic angles for reasons of greater circle rigidity, accuracy and redundancy. It is noted that two telescope sections of the original GAIA with a total of 12 curved mirrors are required for a minimum mission. All these mirror must be kept adjusted and monitored relative to each other. One GAIA95 telescope, however, consists of only 2 curved mirrors, a small field lens, a prism, and 4 flat mirrors, counting the beam combiner as 2 flats. The collecting aperture and the theoretical astrometric performances of the two are nearly the same.

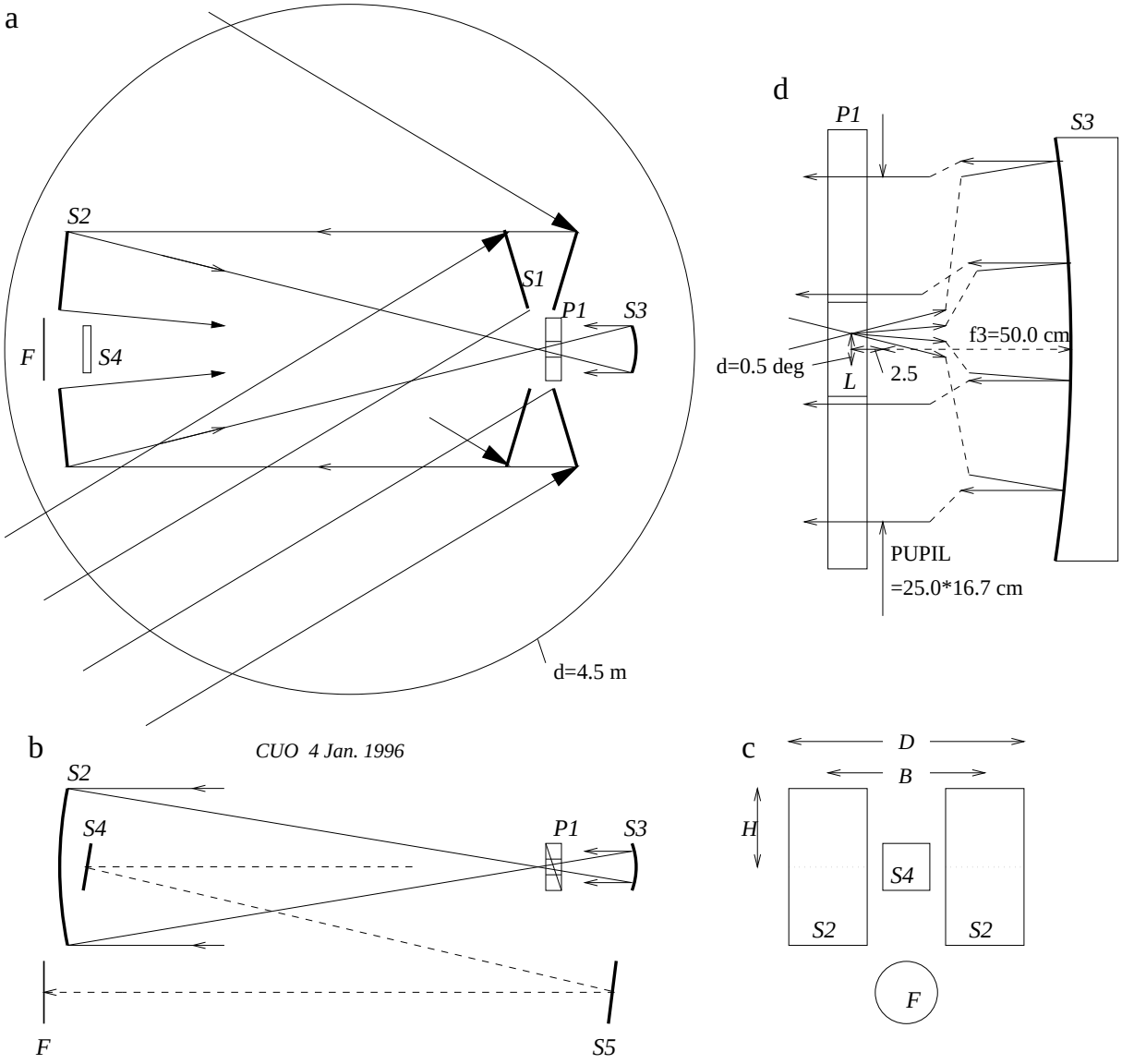

Figure 1: Optical layout of a telescope unit — effective focal length 60 m. (a) Top-view: Hipparcos-type beam combiner, S1, with an aplanatic Gregorian telescope S2-S3, (b) side-view of telescope without beam combiner. The folding mirrors S4 and S5 are used to eliminate astigmatism and distortion. (c) end-view, (d) the prism P1, lens L, and mirror S3, assuming f2=300 cm, S3-F=1050 cm, giving a magnification of 20; the ray tracing after L and the exit pupil are shown as if L were not present, but the field lens in fact shifts the pupil to a position 52 cm behind S3.

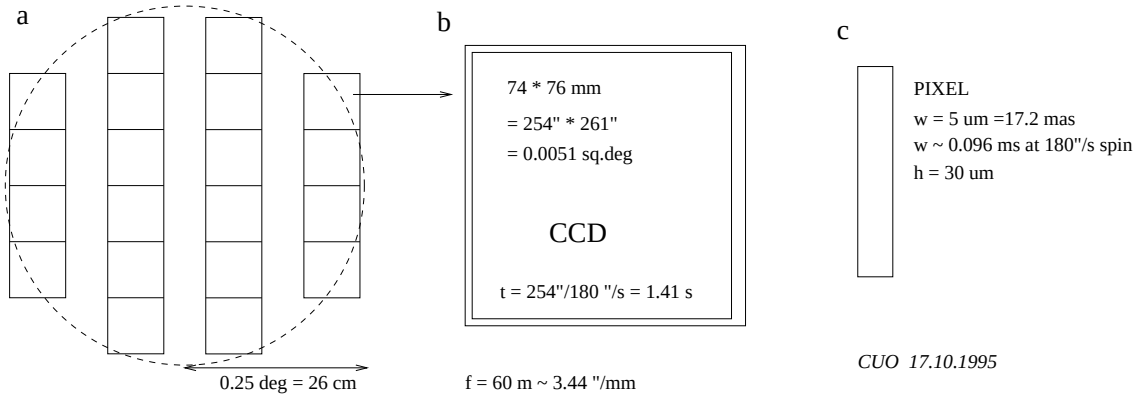

Figure 2: Focal plane layout – $f = 60$ m, scale 3.44 "/mm. (a) The 20 CCDs widely spaced to allow electrical connections, (b) a CCD, (c) a pixel $5 \times 30 \mu m^2$.

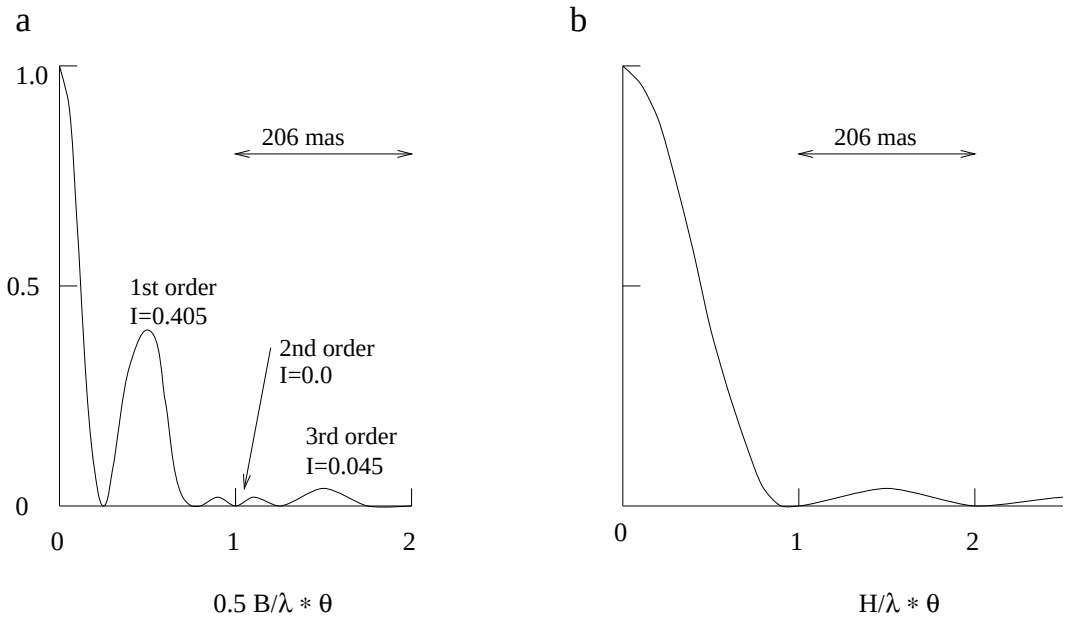

Figure 3: Diffraction patterns of monochromatic light for (a) the direction of scan, i.e., horizontal direction in the figures, (b) the vertical direction. – The abscissa unit is 206 mas at $\lambda = 500$ nm for (a) $B = 100$ cm and for (b) $H = 50$ cm.

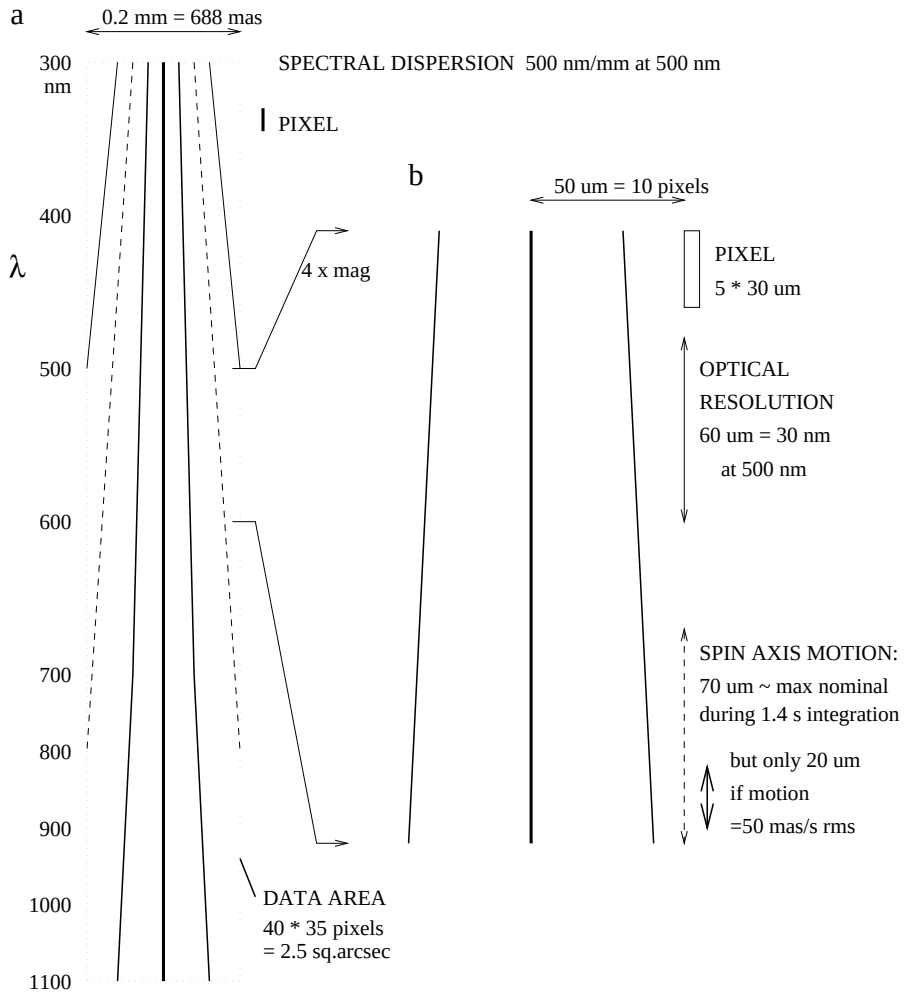

Figure 4: Dispersed fringes. (a) The fringes in the sensitivity range of CCDs, (b) optical and spectral resolution and effect of spin axis motion. We have indicated the variation of dispersion in optical glass, very simplified, by the bend of the 1st order fringe at $\lambda 700$ nm, assuming constant dispersion of 500 nm/mm for the shorter wavelengths and twice this value for longer waves.

There are four optically active surfaces on the beam combiner which also define the four entrance pupils. Since they are close together they should probably be mounted as a solid unit similar to the Hipparcos beam combiner. Short term variations of the basic angle should probably be monitored by picometer metrology. Variations over time scales longer than the spin period of about two hours are best monitored by the astrometric star observations, by the 360 degree closing condition of the great circle reduction.

With the entrance pupil on the beam combiner, i.e., at the focus of S2, the first telescope becomes telecentric so that the principal ray meets the first focal plane perpendicularly. This brings the advantage that the scale value is insensitive to relative axial shift of S2 and S3. The exit pupil would be at the focus of S3, if we could disregard the (large) effect of the field flattening lens.

The distortion is intrinsically rather small and by proper choice of the two the deformations of S4 and S5 it should be possible to eliminate astigmatism and distortion simultaneously.

The two active surfaces of S2 are perhaps best implemented on one rectangular mirror of 100×150 cm^2, or slightly larger to avoid vignetting.

The unused central parts of S1 and S2 have widths of 50 cm, i.e., about the same as the mirrors S4 and S5 and the focal plane. These could therefore be placed higher up in Figs. 1b-c giving an even more compact telescope without any significant vignetting.

The prism should probably be of the straight-viewing type in order to minimize the field distortion, allthough the refracting angle is only 1 to 2 arcmin. Design of the prism must be based on dispersion and transmissivity of the various available glasses taking into account all astrometric and astrophysical arguments. The focus position will be colour dependent, but this effect is negligible due to the very small focal ratio of the transmitted beam if the thickness is less than 2 cm.

The focussed beam at the primary focus passes through a hole in the prism. The beam reflected from S3 is slightly converging with an f-number $= 40$ towards the focus. Some of this light at the edge of the field could pass through the hole, cf. Fig. 1d, and form faint ghost images of stars. This could not happen if the lens is mounted in a diaphragm large enough to cover the hole. In that case only some light could meet the field lens and contribute slightly to a diffuse background.

2.2. Alternative optical design

An alternative optical design of GAIA has been indicated by Lindegren (1995, priv. comm.) Two separate telescopes of the interferometric type shown in Fig. 1, but without beam combiner, are placed parallel to each other as in the ROEMER+ design (Høg 1995a). The two directions of view are realized by means of an inclined plate in front of each telescope, i.e., by one half of the beam combiner in Fig. 1. The advantage would be that stars from the two directions are not superposed in one field of view as they are in Hipparcos and GAIA95. This problem is however small in GAIA95 because the instantaneous field of view is more than a hundred times smaller than in Hipparcos. The disadvantage of the design is that the angles of some mirrors in the two telescopes must be accurately monitored by metrology with respect to relative variations during time intervals smaller than two hours, the spin period of the satellite.

The design solves the possible problem of manufacturing the large beam combiner for GAIA95, and it does not suffer from the problem of GAIA94 that all pathlengths must be carefully controlled in order to maintain fringe visibility.

3. DETECTOR SYSTEM

Large scale CCDs are chosen as detectors, see the focal plane layout in Fig. 2. The CCDs are placed at 6 cm separation to allow sufficient space for electrical connections and radiation protection. The close spacing of CCDs shown for the central part of field for the original GAIA is avoided. Each CCD is placed on placed on a chip about 8×8 cm^2 and contains 15000×2500 pixels of the size 5×30 μm^2. This is beyond the present state of art but is perhaps feasible for a future ESA satellite. The resulting integration time per star is 1.41 s at an assumed spin rate of 180" per second.

The question of readnoise is discussed in Sect. 5.1

4. DISPERSED FRINGES

The monochromatic diffraction images in horizontal and vertical direction are shown in Fig. 3 as function of the angle Θ from the center of the image corresponding to the square pupils shown in Fig. 1c. The two-dimensional monochromatic diffraction image is shown in Fig. 5.

The 0th and 1st order fringes in the horizontal direction, cf. Fig. 3a, contain 90 percent of the light. The second and other even order fringes are cancelled because the pupils have the same width as the dark space between them. The remaining so-called half-fringes of 2nd order are visible in Figs. 3a and 5. The 3rd order fringes are 3.4 mag fainter than the central fringe, but has the same width. This provides a useful attenuation for bright stars and a photometric scale value which may be used for faint stars.

The dispersed fringes are shown in Fig. 4a up to the 3rd order. The dispersion is 500 nm/mm at λ500 nm and is here for simplicity assumed to be completely constant in two ranges of wavelength. The dispersion is produced by the prism P1 which should probably be a straight viewing one in order to minimize the field distortion. The prism acts on the nearly parallel beam reflected from S3. It is located close to the primary focus and a hole in the prism allows the diverging beam to pass unaffected.

The range of wavelengths shown corresponds to the sensitivity range of CCDs, but almost 80 percent of the detected photons from a G0 spectral type star come from the range 400-800 nm. This has been taken into account in the performance calculation below.

The pixel size is matched to the optical resolution in both directions, as seen on Fig. 4b. There are 6 pixels or samples per fringe period in horizontal direction at λ500 nm. This will ensure very little loss of astrometric precision due to undersampling.

4.1. Spectrophotometry and spin axis motion

In vertical direction there is, however according to Fig. 4b, slightly more undersampling since the pixel length is equal to half the optical resolution at λ500 nm. Furthermore, a smearing larger than the optical resolution would occur due to spin axis motion at some parts of the spin, if no precaution is taken. We assume the same spin axis characteristics as for ROEMER. The spin axis motion is nominally 4.1 degree/day corresponding to a 73 day period for the precession of the spin axis about the sun and an angle of 55 degrees between spin axis and sun. During the integration time of 1.41 s this will create a motion as indicated in the lower right corner of Fig. 4 where also the effect of a smaller motion is shown. The smaller motion should ideally not exceed 50 mas/s rms. The spin axis could for instance stay fixed furing 30 minutes (a quarter revolution) and then be moved 308" onto the nominal attitude. If this 'jump' in attitude is allowed to take 20 s the average speed of the spin axis during the time would be only 15 "/s and the power consumption (cold gas) for the accelerations might be acceptable.

With such a spin axis jumping the spectral resolution is 30 nm at λ500 nm corresponding to the width of intermediate bands in photometry. This was recommended for astrophysical reasons by Pel in A7 of SP-379 and by Straižys & Høg in C2 and C13.

4.2. Data sampling

The data area indicated in Fig.4a of 40*35 pixels contains nearly all stellar information. The location of this area for a star requires combined knowledge of satellite attitude and stellar position within about 100 mas rms in both directions. This knowledge is not available at the time of observation where up to 1 arcsec uncertainty should be allowed for the position of an ordinary program star and about 100 mas for the attitude, according to van Leeuwen (priv. comm.) It appears from the figure that data must be read from the CCD in a 4 times wider area and slightly higher. An onboard detection of the central fringe is then required to narrow the area along the scan direction. For the purpose of spin axis attitude determination in real time a detection of the vertical position of the image is required for a million attitude stars brighter than $V = 11$ mag with accurately known positions. The Tycho Catalogue will serve this purpose well. The vertical position might be detected by the K-line in a large number of stars and by the intensity fall-off at the ends of the spectrum, provided a spectral type is known.

5. PERFORMANCE

The astrometric precision inherent in a diffraction image due to photon noise was derived by Lindegren (1978). These formulae are given below in Eqs.(5-7), but first we give the formulae for optical resolution, thus facilitating a comparison.

The angular resolution at the wavelength λ for a circular aperture of diameter D is

$$\Delta\Theta = 1.22\lambda/D \qquad (1)$$

defined as the radius of the first dark diffraction ring.

Similarly, for a slit pupil of width b the distance from center of the diffraction image to the first minimum is

$$\Delta\Theta = \lambda/b \qquad (2)$$

For a double slit pupil of baseline B (center-to-center distance) and independent of slit width the first minimum in the interference pattern is at the distance

$$\Delta\Theta = \lambda/2B \qquad (3)$$

and the pattern itself has a first minimum given by Eq.(2), see Fig. 3a illustrating the special case where $B = 2b$ and $b = H$.

The formulae for the one-dimensional position error of a stellar image are similar to those for the optical resolution, though with subtle differences in the coefficients. The following formulae give the standard errors for an image containing N recorded photons. For a circular pupil without central obscuration we have

$$\sigma_N = \frac{\lambda}{\pi D\sqrt{N}} \ , \qquad (4)$$

for a rectangular pupil of width L:

$$\sigma_N = \frac{\lambda}{1.155\pi L\sqrt{N}} \ , \qquad (5)$$

and for an interferometer with baseline B between two pupils:

$$\sigma_N = \frac{\lambda}{2\pi B\sqrt{N}}. \qquad (6)$$

The real measurement error will be larger for instance due to undersampling of the image and perhaps optical aberrations, but this is not taken into account in the present report.

We will consider an interferometer with two rectangular pupils of width b and therefore the total pupil width $L = B + b$ in order to derive the value of b which gives the best astrometric precision for a fixed value of L.

The pupil height H is not relevant and is set to unity. The total collecting aperture has the area $A_c = 2Hb$. It follows from (6) that the error is proportional to

$$\sigma = \frac{1}{(L-b)\sqrt{b}}. \qquad (7)$$

This formulae is only approximately correct since we see from Eq.(5) that Eq.(6) gives an error 15.5 percent too large for an interferometer without spacing between the two rectangular pupils. But we are not interested in this extreme case.

The error (7) obtains a minimum for $b = L/3$, i.e., when the single pupil width is equal to the space between the pupils. This geometry is therefore selected for our interferometer.

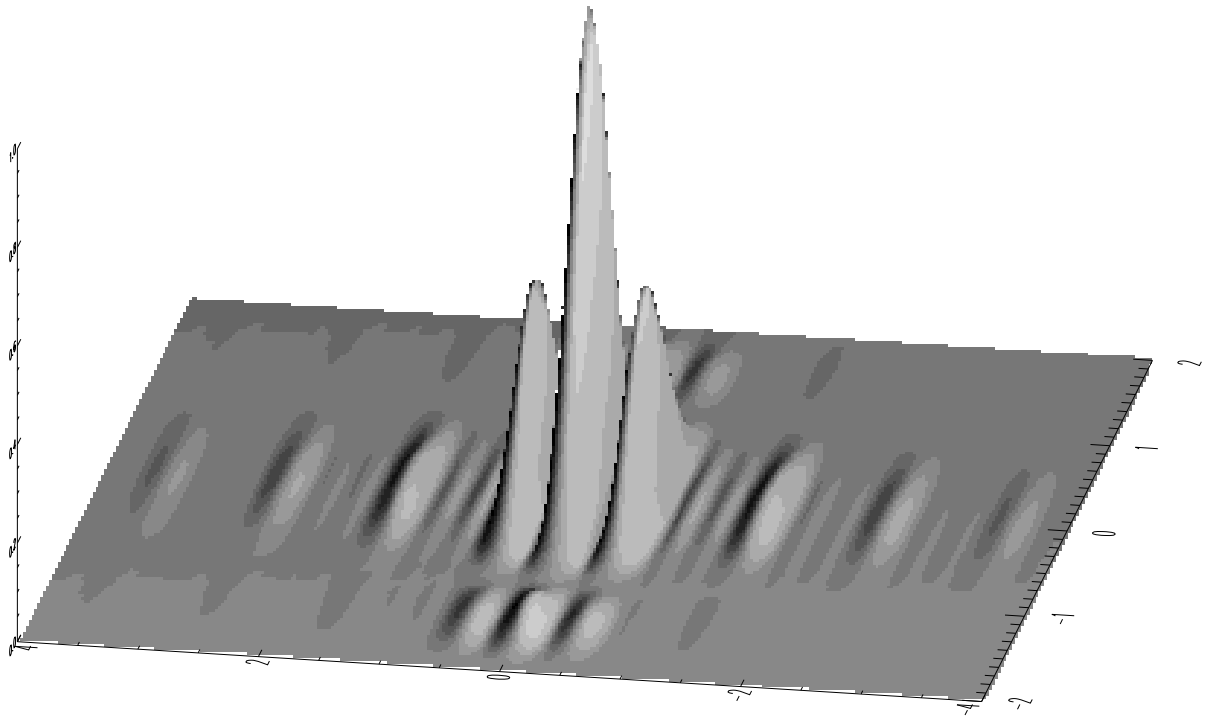

Figure 5: *The two-dimensional monochromatic diffraction image, cf. Sect. 4, Fig. 3.*

Table 1: Two telescope units of the new design with 100 cm baseline using dispersed fringes, 5 year mission. Predicted standard errors due to *photon noise* in astrometry and photometry for a G0-star, cf. Sect. 5.1. The effects of e.g., background, readnoise and undersampling are included. Units: mas = milliarcsec, and 10 nm for the 8 central wavelengths in line #3.

	Astrometry		Photometry [millimagnitude]								
V	par.	p.m.	W	u	P	v	b	Z	y	S	I
mag	mas	mas/year		35	37	41	47	52	55	66	81
12	0.003	0.002	0.1	1	1	1	1	1	1	1	1
14	0.008	0.005	0.2	3	2	2	1	1	1	1	1
16	0.022	0.013	0.6	7	6	4	3	3	3	3	1
18	0.068	0.040	1.6	24	20	12	9	8	8	9	3
20	0.302	0.177	6.3	70	60	30	25	20	20	20	9

Table 2: Global astrometric standard error for a star of $V = 15$ of some proposed missions, cf. Sect. 5.2. The two last columns give astrometric standard errors calculated by Eq. (8) with the parameters of the preceding columns, and the error given by the author of the mission proposal.

Proposed mission	Parameters of the mission						σ	
	N_f	A_c	A_d	T	D	B	Eq. (8)	Author
		m^2	$\square^\circ$	yr	cm	cm	mas	mas
Original GAIA, direct fringe detection	3	.39	.32	5	-	250	.0038	.003
Original GAIA, incoherent image det.	3	.39	.43	5	50	-	.033	.033
GAIA95, dispersed fringe det.	4	.50	.10	5	-	100	.013 $\equiv$	.013
FAME, dispersed fringe det.	2	.04	.046	2.5	-	40	.33	.66

5.1. Performance of GAIA95

The precision for a G0 star due to photon noise of a 5 year mission with two GAIA95 telescopes is given in Table 1. The table contains the standard errors for parallax, annual proper motion and photometry.

The photometric precision is given for magnitudes in a wide band W from the whole spectral sensitivity of the CCD, and for the 8-band Stromvil+I system proposed by Straižys & Høg in C2 and C13 of SP-379. The central wavelength for the 8 bands is given in units of 10 nm in line #3. The 7 intermediate bands should have width (FWHM) about 25 nm from an astrophysical point of view. The infrared band I should have the larger width 166 nm so that the smaller spectral dispersion of optical glasses at long wavelengths, cf. Fig. 4a, poses no problem. The spectrophotometric precision is better than for the original GAIA (Table 2 of I2 in SP-379) in spite of the smaller light collecting aperture because all light is used from all wavelengths, not only that passing a particular colour filter.

Realistic assumptions were made for mirror reflectivities, for the QE of thinned CCDs and for the mission deadtimes. A readnoise of effectively 1 e- per pixel was assumed which by far dominates any reasonable assumptions about sky background and scattered light. The assumed readnoise is lower than present state of art but a reasonable projection for the distant future of a satellite. Jorden & Oates (1995) expect that 5 e- noise at 1 MHz pixel rate will be obtained within a few years. In any case it appears that readnoise is a critical parameter of the CCD. An ideal readnoise of zero would decrease the astrometric errors given in the table by 5, 20 and 40 percent at $V = 16$, 18 and 20, respectively.

We shall now discuss a method to decrease the effective readnoise if required. For stars fainter than $V = 14$ the astrometric and photometric precision would be hampered if we assume, for example, a readout noise of 8 e- per pixel in case all pixels of the data area are read individually. This takes 2 μs per pixel since about 50 pixels in a vertical column of the data area have to be read in the 96 μs available, cf. Fig. 2c. This problem is partly solved by adding 2, 3 or more consecutive pixels in vertical direction during the readout. The number of pixels to be added is function of the magnitude given in the input catalogue. If 4 pixels are added the available time would be 8 μs per sample with a readnoise of 6 e- per sample. This corresponds to 3 e- per original pixel. The resulting smearing of horizontal resolution would be negligible even for much larger numbers than 4 pixels.

This addition of pixels means less loss of astrometric precision due to readnoise than if pixels are read individually, but the photometric bandwidth is widened to about 60 nm which should be acceptable for faint stars.

It takes time to skip the unwanted pixels in a vertical row during the 96 μs available, but this has not been taken into account here. It is expected that multiple outputs from each CCD would solve the problem.

5.2. Comparison of astrometric missions

Formulae shall be given for comparison of performances of various astrometric mission proposals in another more independent way than by tables similar to Table 1 given by the various authors.

We can write the number of collected photons per star with a given instrument as

$$N = cN_f A_c A_d T \tag{8}$$

where c is a constant of proportionality, N_f is the number of fields-of-view, for instance $= 2$ for Hipparcos and $= 3$ for the original GAIA with 3 sections. Furthermore, A_c in [m^2] is the collecting aperture per field, A_d in [sq.deg] is the angular area of detectors per field, and T in [yr] is the mission length.

The Eqs.(4-6) may be used with N from Eq.(8) for approximate comparison of different satellite designs. In this form the equations do not take into account the stellar magnitude or possible different quantum efficiencies of the detectors, or effects of instrument absorption, undersampling, background noise or readout noise — which require separate discussion.

The result of comparing the original GAIA, GAIA95 and FAME missions is given in Table 2. A constant $c = 3740$ for Eq.(8) is obtained by adopting the parallax error 0.013 mas for $V = 15$ from a GAIA95 mission with zero readnoise.

It appears that fair agreement is found between the precision given by means of Eq.(8) and that given for the original GAIA by Lindegren & Perryman in Tables 1 and 2 of I2. For FAME the value for $V = 15$ is derived as 10 times the error at 100 times brighter stars given in the FAME report and is therefore unaffected by readnoise. The value 0.66 mas is 2.0 times the value from Eq.(8), probably because the value given by FAME takes undersampling and other non-ideal conditions for FAME into account.

6. CONCLUSIONS

The expected performance of the new design given in Table 1 is preliminary and believed to be on the conservative side. It would be improved if for instance the CCDs can be packed more densely than shown in Fig. 2a, and if a larger field with CCDs may be used. The beam combiner and primary mirror and thus the interferometer baseline may be larger than assumed here. If for instance the dimensions B, D, H are multiplied by the factor g the theoretical errors will be multiplied by a factor g^{-2}, according to Eqs. (6) and (8). If only the baseline is multiplied by g without a change of collecting aperture the errors will be multiplied by a factor g^{-1}, according to Eq. (6). Optical calculations of the telescope are required before we can go deeper into such possibilities. Especially the remaining aberrations after removal of field astigmatism and field curvature must be studied. Altogether a precision of 4 microarcsec for parallaxes at $V = 14$ mag may be possible.

Systematic errors of the astrometry and spectrophotometry should be studied. The problems of CCD photometry, e.g. the variation of spectral sensitivity from pixel to pixel have been discussed by Young (1995).

The scientific impact of the fainter limiting magnitude with interferometry than the original GAIA and the better resolution of crowded areas, minor planets, double and multiple stars and quasars, should be very significant.

7. CHANGES

Changes in the issue of **8 Dec 1995** of this report compared to previous ones:

Figs 1a-c: The oversizing of mirrors S4, S5 and S6 has been reduced.

Section 2.1: New paragraph is "The unused para..." (about a more compact telescope.)

Section 2: New comments on axial astigmatism and on field curvature.

Changes in the issue of **4 Jan. 1996** of this report compared to the previous one:

Section 2: An aplanatic Gregorian system replaces the Gregorian of two Wright-Vaisala systems. This greatly facilitates the manufacture of the beam combiner because it consists now of simple flats, not with any elliptical deformation. Furthermore, the basic angle may be larger, e.g. 80 degrees. — Fig. 1b: the tilted mirrors S4 and S5 replace the previous S4, S5 and S6.

ACKNOWLEDGEMENTS

The authors are grateful for useful discussions with Drs. P. K. Seidelmann, M. Shao and J. P. McGuire on the FAME project and for access to information on the project in advance of publication. We gratefully acknowledge comments to a previous version of this paper by Drs. L. Lindegren and M. A. C. Perryman, and we thank Drs.C. Dainty and J. Maxwell from Imperial College, London, for some very valuable comments on the telescope system. This work was supported by the Danish Space Board.

REFERENCES

Bahner K. 1967, Teleskope, in Handbuch der Physik, Band XXIX, 227, Springer-Verlag, Berlin-Heidelberg-New York.

Casertano S. 1995, Science and Technology: Trade-Offs in the Design of a Future Astrometric Mission. E2 of ESA SP-379.

Daigne G. 1995, Direct Fringe Detection and Sampling of the Diffraction Pattern, C6 of ESA SP-379.

ESA SP-379 1995, *Future Possibilities for Astronomy in Space*, by M.A.C. Perryman and F. van Leeuwen (eds.), a workshop at RGO, Cambridge, England, 19-21 June 1995, ESA Publications Division, ESTEC

Gai M., Lattanzi M.G., Casertano S. & Guarnieri M.D. 1995, Non-Conventional Detector Applications for Direct Focal Plane Coverage, C10 of ESA SP-379.

Høg E. 1993, Astrometry and photometry of 400 million stars brighter than 18 mag, in: *I.I. Mueller and B. Kołaczek (eds.) Developments in Astrometry and Their Impact on Astrophysics and Geodynamics, IAU Symp. No. 156*, 37.

Høg E. 1995a, A new era of global astrometry. II: A 10 microarcsecond mission, in E. Høg and P.K. Seidelmann (eds.) *Astronomical and Astrophysical Objectives of Sub-milliarcsecond Optical Astrometry*, IAU Symposium No. 166, Kluwer Academic Publishers, Holland, 317.

Høg E. 1995b, Three Astrometric Mission Options and a Photometric System, C13 of ESA SP-379.

Johnston K. (principal investigator) 1995, Fizeau Astrometric Mapping Explorer (FAME), Step 1 Proposal to NASA.

Jorden P.R. & Oates A.P. 1995, Scientific CCD Prospects for 1994 and Beyond, in A.G. Davis Philip *et al.* (eds.) IAU Symposium No. 167, Kluwer, p. 27.

Lattanzi M.G. 1995, Summary of the Parallel Session, E5 of ESA SP-379.

Lindegren L. 1978, In F.V. Prochazka and R.H. Tucker (eds.), *Modern Astrometry*, IAU Coll. No. 48, p. 197.

Lindegren L. 1995, Summary of the Parallel Session, C15 of ESA SP-379.

Lindegren L., Perryman M.A.C., Bastian U., Dainty J.C., Høg E., Kovalevsky J., Labeyrie A., van Leeuwen F., Loiseau S., Mignard F., Noordam J.E., Le Poole R.S., Thejll P., Vakili F. 1994, GAIA - Global Astrometric Interferometer for Astrophysics, in J.B. Breckenridge (ed.) *Amplitude and Intensity Spatial Interferometry II*, SPIE Conference Proceedings, Vol. 1947, p. 147

Lindegren L., Perryman M.A.C. 1994, A Small Interferometer in Space for Global Astrometry: The GAIA Concept, IAU Symp. No. 166, p. 337.

Lindegren L., Perryman M.A.C. 1995, The GAIA Concept, I2 of ESA SP-379.

Mignard M. 1995, Highlights of the Hipparcos Mission, I1 of ESA SP-379.

Makarov V.V., Høg E., Lindegren L. 1995, Random errors of star abscissae in the ROEMER space astrometry project, in press in: *Experimental Astronomy.*

Noordam J.E. 1995, On the Advantages of Dispersed Fringes, C7 of ESA SP-379.

Pel J.W. 1995, Some Thoughts about the Photometric System of GAIA, A7 of ESA SP-379.

Schroeder D.J. 1987, Astronomical Optics, Academic Press, Inc., London.

Seidelmann P.K., Johnston K.J., Urban S. *et al.* 1995, A Fizeau Optical Interferometer Astrometric Satellite, C1 of ESA SP-379.

Straižys V., Høg E. 1995, An Optimum 8-Colour Photometric System for a Survey Satellite, C2 of ESA SP-379.

Young A.T. 1995, Choosing Filters to make CCD Photometry Transformable, in A.G. Davis Philip *et al.* (eds.) IAU Symposium No. 167, Kluwer, p. 145.